



Unveiling Interindividual Variability of Human Fibroblast Innate Immune Response Using Robust Cell-Based Protocols

Audrey Chansard^{1†}, Nelly Dubrulle^{1†}, Mathilde Pujol de Molliens^{1†}, Pierre B. Falanga¹, Tharshana Stephen², Milena Hasan², Ger van Zandbergen³, Nathalie Aulner¹, Spencer L. Shorte^{1,4*}, Brigitte David-Watine^{1,5,6,7,8*} and the Milieu Intérieur Consortium

OPEN ACCESS

Edited by:

Thomas A. Kufer,
University of Hohenheim, Germany

Reviewed by:

Saadia Kerdine-Römer,
Université Paris-Sud, France
Sandra Stephanie Diebold,
King's College London,
United Kingdom

*Correspondence:

Brigitte David-Watine
brigitte.david-watine@pasteur.fr
Spencer L. Shorte
spencer.shorte@pasteur.fr

†These authors have contributed
equally to this work

Specialty section:

This article was submitted to
Molecular Innate Immunity,
a section of the journal
Frontiers in Immunology

Received: 03 June 2020

Accepted: 19 November 2020

Published: 11 January 2021

Citation:

Chansard A, Dubrulle N, Pujol de Molliens M, Falanga PB, Stephen T, Hasan M, van Zandbergen G, Aulner N, Shorte SL, David-Watine B and the Milieu Intérieur Consortium (2021) Unveiling Interindividual Variability of Human Fibroblast Innate Immune Response Using Robust Cell-Based Protocols. *Front. Immunol.* 11:569331. doi: 10.3389/fimmu.2020.569331

¹UTechS Photonic BiImaging, C2RT, Institut Pasteur, Paris, France, ²UTechS Cytometry and Biomarkers, CRT, Institut Pasteur, Paris, France, ³Division of Immunology, Paul-Ehrlich-Institut, Federal Institute for Vaccines and Biomedicines, Langen, Germany, ⁴Pasteur Joint International Research Unit Ai3D, Institut Pasteur Korea, Seongnam-si, South Korea, ⁵Unité INSERM U 1223, Institut Pasteur, Paris, France, ⁶Unité Biologie et Génétique de la Paroi Bactérienne, Institut Pasteur, Paris, France, ⁷CNRS UMR2001, Paris, France, ⁸INSERM, Équipe Avenir, Paris, France

The *LabEx Milieu Interieur (MI)* project is a clinical study centered on the detailed characterization of the baseline and induced immune responses in blood samples from 1,000 healthy donors. Analyses of these samples has lay ground for seminal studies on the genetic and environmental determinants of immunologic variance in a healthy cohort population. In the current study we developed *in vitro* methods enabling standardized quantification of MI-cohort-derived primary fibroblasts responses. Our results show that *in vitro* human donor cohort fibroblast responses to stimulation by different MAMPs analogs allows to characterize individual donor immune-phenotype variability. The results provide proof-of-concept foundation to a new experimental framework for such studies. A bio-bank of primary fibroblast lines was generated from 323 out of 1,000 healthy individuals selected from the MI-study cohort. To study inter-donor variability of innate immune response in primary human dermal fibroblasts we chose to measure the TLR3 and TLR4 response pathways, both receptors being expressed and previously studied in fibroblasts. We established high-throughput automation compatible methods for standardized primary fibroblast cell activation, using purified MAMPS analogs, poly I:C and LPS that stimulate TLR3 and TLR4 pathways respectively. These results were in turn compared with a stimulation method using infection by HSV-1 virus. Our “Add-only” protocol minimizes high-throughput automation system variability facilitating whole process automation from cell plating through stimulation to recovery of cell supernatants, and fluorescent labeling. Images were acquired automatically by high-throughput acquisition on an automated high-content imaging microscope. Under these methodological conditions standardized image acquisition provided for quantification of cellular responses allowing biological variability to be measured with low system noise and high biological signal fidelity. Optimal for automated analysis of immuno-phenotype of

primary human cell responses our method and experimental framework as reported here is highly compatible to high-throughput screening protocols like those necessary for chemo-genomic screening. In context of primary fibroblasts derived from donors enrolled to the MI-clinical-study our results open the way to assert the utility of studying immune-phenotype characteristics relevant to a human clinical cohort.

Keywords: immortalization, HSV-1, FACS, cytokines, human primary cells, NF- κ B, TLR (Toll like receptors), innate immunity

INTRODUCTION

The *LabEx Milieu Interieur (MI)* project (www.milieuinterieur.com) is a clinical study aiming to provide the first description of both genetic and environmental determinants of immunologic variance within the general healthy population (1). Central to this study, blood samples from healthy volunteers were stimulated by a range of 40 distinct stimuli allowing to characterize the induced immune response (*i.e.* major secreted cytokines chemokines, transcriptome *etc.* 2–4). As part of the MI-program skin biopsies were collected from 323 out of 1,000 healthy individuals and primary human fibroblasts were prepared (Genethon, Evry, France). The MI-fibroblasts collection (323 primary fibroblasts) comprises a one-of-a-kind cell collection inasmuch as each derived primary cell isolate is uniquely associated with its corresponding donor data in the *LabEx MI* genotype-to-phenotype database (e.g. serology, genomic/proteomic analysis, microbiota, clinical data, and epidemiological selection criteria).

Fibroblasts are the principal cellular constituents of connective tissues. Functionally fibroblasts can be described as a population of cells that synthesize and secrete a complex array of structural and non-structural extra-cellular matrix (ECM) molecules. Fibroblasts actively organize and remodel ECM through the production of proteinases, and converse with nearby cells through paracrine, autocrine and other forms of communication (5). As such fibroblasts are fundamental to tissue homeostasis and normal wound repair. The role of fibroblasts in the defense against pathogens and more generally in innate immunity has only recently emerged with the discovery of Toll-like receptors (TLRs; 6). The TLRs family consists of more than 13 prototype pattern-recognition receptors (PRRs) that recognize microbial-associated molecular patterns (MAMPS) from various microbial pathogens such as viruses, bacteria, protozoa and fungi or from danger-associated molecular patterns (DAMPS) from damaged tissue (7, 8). Moreover, dominant producers of interleukin-6 (IL-6) at sites of peripheral inflammation, fibroblasts are now recognized for their major contribution to inflammatory regulation (9, 10). Fibroblasts are emerging with a key role in local innate immunity evoked during response to pathogens as well as vaccines (11–14).

The *LabEx MI* program highlighted the value of developing and systematically using standardized methodologies for measuring blood host immune responses. The systematic standardization of blood sample preparation and handling protocols enabled an

unprecedented measure of inter-individual phenotype variance relevant to the human population cohort. Particularly, MI-studies showed that the whole blood stimulation by different MAMPs analogs are more informative to reveal the individual variability than unstimulated samples (2, 15).

Our MI-program experience raised the fundamental question of whether the MI-fibroblast collection might also present innate immune response characteristics relevant to studying inter-individual donor variance. The first step to address this question requires to validate methods and protocols allowing to characterize and quantify the inter-individual variance of the innate immune response of the donor primary fibroblast collection.

That TLR3 and TLR4 receptors are integral to innate immune response in fibroblasts is supported by numerous studies (16, 17). Further, deficits in the TLR3 pathway are associated with cases of herpes viral encephalitis in young children and can be identified *in vitro assay* with patient's fibroblasts (18–20). We therefore hypothesized that TLR3/TLR4 variability in the MI-population cohort should be detectable *in vitro* and might therefore provide an insightful measure of inter-individual variance preserved in fibroblasts of the MI-study. In a first step toward investigating such a phenomena in a high-value asset primary human cell collection comprising over three-hundred unique donor primary fibroblasts we report here the development of two standardized assays:

1. HSV-1(Herpes Simplex Virus type 1) infection: monitoring of the cell response were developed and tested by using cells harboring mutations in the TLR3 pathway. HSV-1 is an ubiquitous human neurotropic virus that affects up to 85% of the world's population with recurrent clinical HSV-1 infections and manifestations (21, 22). HSV-1 is recognized by different TLRs: TLR2 for surface viral structures, TLR3 for dsRNA, and TLR9 for viral DNA (23).
2. MAMPS analogs stimulation: the TLR3 ligand of choice is polyinosinic-polycytidilic acid (poly I:C), a synthetic analog of double-stranded RNA (dsRNA), a MAMP associated with viral infection. On the other hand TLR4 is stimulated by lipopolysaccharide (LPS), a MAMP associated with the major structural component of the outer wall of all Gram-negative bacteria.

After recognition of MAMPs, TLRs recruit a cascade of adaptor proteins by homophilic protein-protein interactions *via* their TIR-domains (Toll/interleukin-1 receptor/resistance protein domain) leading to the activation of transcription factor nuclear factor-kappa B (NF- κ B). Accordingly, both

TLR3 and TLR4 pathways lead to translocation from the cytoplasm to the nucleus of the transcription factor NF- κ B, albeit with different kinetics and *via* distinct protein-protein signaling cascades. The early phase of NF- κ B activation depends on the MyD88-dependent pathway and the late phase NF- κ B activation is controlled by the TRIF-dependent pathway (7). We therefore reasoned visual detection of NF- κ B nuclear translocation can be used to quantify TLR3/TLR4 activation. Accordingly, we developed an “Add-only” protocol to avoid signal variability resulting from medium exchange. We validate the protocols for poly I:C and LPS stimulation by comparing responses in a subset of MI-donor primary fibroblasts (13 of the 323), to measurements performed on MI-extraneous immortalized fibroblasts lines from patients with mutations in the TLR3 or TLR4 pathways, and commercially supplied primary fibroblasts from single donors.

Hereby we describe our highly standardized protocols for stimulation/infection of primary human fibroblasts and the measurement of their immune response signatures at cellular and protein level which has enabled the identification of high and low fibroblast-specific responses to LPS.

MATERIALS AND METHODS

Reagents

For infection experiments, we used a HSV-1 in which GFP (green fluorescent protein) was fused to a viral capsid protein (VP26) (strain KOS (24)). A high concentration stock of HSV-1-GFP was a generous gift from Prof. Desai (Virology Laboratories, Department of Pharmacology and Molecular Sciences, Johns Hopkins University School of Medicine, Baltimore, Maryland).

Poly I:C (High molecular weight), a synthetic analog of double-stranded RNAs that binds to the TLR3 receptor, and LPS (LPS-EB Ultrapure E.coli 0111: BA), a component of the gram-negative bacterial membrane that binds to the TLR4 receptor were purchased from Invivogen.

Human TNF α premium grade was from Miltenyi Biotec and Interferon α -2b INTRONA from Merck MSD France.

Cells and Donors

DHF primary fibroblasts (women, 55 years old, Causasian, Zenbio Inc.) were purchased at Tebu, France. BJ (CRL-2522) and WI-38 (CCL-75) human fibroblasts were from ATCC.

The following SV40-immortalized fibroblasts were provided by J-L. Casanova, Laboratoire de génétique humaine des maladies infectieuses, Université Paris Descartes: TLR3^{-/-} (25), 2018 (TLR3^{+/-}) and 1323 (TLR3^{+/-}) (20), TRIF^{-/-} (18), TBK1^{+/-} (26), Nemo^{-/-} (27) from patients and two control fibroblasts from healthy donors, C65 and C72.

LabEx MI primary fibroblasts were prepared from biopsies of the non-sun exposed interior of the arm of healthy volunteers at the Genethon (Evry, France). The identity of the subjects is coded by a number. The following numbers: 209, 220, 221, 241, correspond to women age 30–39; 318, 323, 341, 376 to men age 30–39; 818, 819, 820 to women age 60–69; and 914, 915: men age

60–69. Biopsies were obtained from a subset of the *LabEx MI* healthy donor cohort, approved by the *Comité de protection des personnes* – Ouest 6 (Committee for the protection of persons) on June 13th, 2012 and by the French Agence nationale de sécurité du médicament (ANSM) on June 22nd, 2012. The study is sponsored by Institut Pasteur (Pasteur ID-RCB Number: 2012-A00238-35) and was conducted as a single center interventional study without an investigational product. The original protocol was registered under ClinicalTrials.gov (study# NCT01699893). The samples and data used in this study were formally established as the Milieu Interieur biocollection (NCT03905993), with approvals by the Comité de Protection des Personnes – Sud Méditerranée and the Commission nationale de l'informatique et des libertés (CNIL) on April 11, 2018.

Cell Culture

The cells were cultured in DMEM GlutaMAX (Dulbecco's Modified Eagle Medium, Life Technology) supplemented with 10% FCS (fetal calf serum, Life Technology) without antibiotics. The cells were incubated at 37°C, 5% CO₂. Primary fibroblasts were passaged at 70-80% confluency. The cells are said to pass $n + 1$ each time they are detached by trypsinization and seeded again in new culture flask with fresh medium. For primary dermal human fibroblasts, one passage corresponds in average to the multiplication by three of the cell population over a period of one week. Routinely, the cells were analyzed between passage 5–6 and passage 10.

Cells were regularly assessed for mycoplasma contamination by using the Mycotest kit (Enzo).

Infection With Herpes Simplex Virus-1

At day 1, the cells were plated in a 96-well plate (μ Clear Bottom, Greiner CAT 655090): 12,000 cells per well for primary fibroblasts and 6,000 cells per well for fibroblast lines immortalized in 50 μ l of cell culture medium. The cells were incubated for 24 h before being infected at different multiplicities of virus (MOI) (0.01, 0.05, 0.1, or 0.5 MOI) in DMEM at 2% FCS. The virus was left in contact with the cells for 2 h, then was replaced by complete DMEM medium at 10% FCS. The cells were then incubated for a further 24 h at 37°C and 5% CO₂. The cells were then fixed in 4% PFA (Electron Microscopy Sciences) for 15 min at room temperature. Finally, the nuclei of the cells were labeled with Hoechst 33342. The GFP fluorescence of the samples were quantified at 24 h after infection.

For assaying cell protection to viral infection, cells were treated with 10⁵ IU/ml IFN α -2b for 18 h before infection.

Protocol “Add-Only” for Poly I:C and Lipopolysaccharide Stimulation

At day 0: The cells were plated in 100 μ l of DMEM 10% FCS in a 96-well plate (Clear Bottom, Greiner): 12,000 cells per well for primary fibroblasts and fibroblast lines and 6,000 cells per well for the immortalized fibroblast lines.

At day 1: Two times concentrated poly I:C: 0.2 μ g, 2 μ g, 10 μ g, and 20 μ g for 1 ml; or two times concentrated LPS: 0.2 μ g, 1 μ g, 2 μ g of LPS for 1 ml, were prepared in DMEM 10% FCS and

100 μ l were added on top of the cells without medium withdrawing so that final concentration is halved.

Incubation time was 3 h for LPS and 24 h for poly I:C for monitoring the expression of NF- κ B.

After 3 h on day 1 for LPS or 24 h on day 2 for poly I:C, twenty-five μ l of PFA 32% are added to the 200 μ l of medium to achieve a final concentration of 3,5%. After 15 min, the cells were carefully rinsed with PBS twice then processed for immunofluorescent labeling.

For cytokine analysis, the supernatants were retrieved 24 h after the beginning of the LPS and poly I:C stimulation and transferred to a plate for freezing. For LPS stimulation, the same experiment is performed in parallel in two 96-plates and one plate is fixed with PFA after 3 h for NF- κ B analysis. For poly I:C stimulation, after removal of the supernatant, the cells are fixed in PBS 4% PFA.

All the steps of this protocol can be easily adapted to automation (data not shown).

Immuno-Fluorescent Labeling

To carry out the immuno-fluorescent labeling, the cells were permeabilized for 15 min in PBS-0.1% Triton (D-PBS, Life Technology). The cells were then incubated for 1 h at room temperature in blocking buffer (PBS- fat dry milk 5%). Then, the cells were incubated with a monoclonal anti-human NF- κ B p65 antibody (27F9.G4, 1/2000, Rockland) diluted in the blocking solution (PBS-milk 5%) overnight at 4°C. Fluorescent anti-mouse secondary antibodies were diluted in the blocking solution and incubated for 2 h at room temperature. Finally, the nuclei were labeled with Hoechst 33342 (0.5 μ g/ml, Invitrogen) for 15 min at room temperature.

Image Acquisition and Analysis

After immunofluorescent labeling of fixed cells, two channel images were acquired in a fully automated and unbiased manner using an automated spinning disk confocal microscope (OPERA QEHS, Perkin Elmer Technologies, UtechS PBI, Institut Pasteur) and a 10 \times air objective (NA=0.4) with the following sequential acquisition settings: (i) 561 nm laser line excitation, filter 600/40 for Cy3 detection, or 488 nm laser line excitation, filter 540/75 for Alexa 488 detection and (ii) 405 nm laser line excitation, filter 450/50 for Hoechst 33342 detection. Forty-seven images per channel, covering roughly the entire surface of each well, were collected for reliable statistical analysis considering potential spatial cell and compound distribution biases.

The images and associated metadata were transferred to the Columbus ConductorTM Database (Perkin Elmer Technologies) for storage and further analysis. The image analysis was performed by batches in Columbus using custom designed image analysis building blocks.

For HSV-1 infection, only the fluorescence intensity in nuclei containing a green fluorescent protein (VP26-GFP) fused capsid protein is considered to identify HSV-1 positive cells. A ratio of cells defined as HSV-1 (GFP) positive is calculated on the total population defined by the number of Hoechst labeled nuclei, which corresponds to the percentage of infected cells on the total population at a certain multiplicity of infection.

To analyze the translocation of NF- κ B in the nucleus, the routine allows to enumerate the total number of cells and to measure the average intensities of fluorescence *per pixel* (or unit area) in the masks considered (the nucleus and the cytoplasm) in each individual cell. A ratio of the fluorescence intensity of the nucleus to the fluorescence intensity of the cytoplasm is calculated: if this ratio is higher at 1.2 we consider that the cells are stimulated, if this ratio is less than 1 we consider that the cells have not been stimulated. We report then the proportion of stimulated cells in the entire population of each well at a given condition to characterize the stimulus level.

Cytokine Flow Cytometry

Cells were stimulated with LPS 1 μ g/ml or poly I:C 20 μ g/ml during 72 h, then treated with brefeldin A 1x (Abcam ab193369) for 6 h. The cells were trypsinized and resuspended in 0,5 ml PBS and fixed by addition of 0,5 ml PBS 8% PAF on ice for 20 min. Fibroblasts were then permeabilized in PBS-SVF 1%, 0,3% Triton X100 for 20 min at 4°C. The cells were labeled in PBS-SVF 1%, 0,1% Triton X100 with anti-huIL-6-FITC (BD Biosciences, 340526) and anti-huIL-8-APC (Miltenyi Biotec, 130-112-015) and analyzed on a Fortessa cytometer in the Cytometry and Biomarkers UtechS, Institut Pasteur.

Cytokine Dosage

Cell culture media were collected post-stimulation at different timepoints and stored at -80°C until further analysis. The thawed samples were centrifuged at 13 000g at 4°C for 10 min. In the undiluted media samples, the cytokine levels were determined by Luminex xMAP technology using Human Custom ProcartaPlex Assay kit (ThermoFisher, Cat PPX-04-MXRWEYU) in accordance with the manufacturer's recommendations. The protocol was adapted to DropArray plate (Clinisciences, Cat 96-CC-BD-05); a luminex method based on the use of a 96 well-plate capable of a five-fold miniaturized format with regards to sample (5 μ L minimum) and Luminex reagents (28). The cytokine levels were measured for a combination of 4 different cytokines: interleukin-6 (IL-6), interleukin-8 (IL-8), interferon α (IFN α) and Monocyte Chemoattractant Protein-1 (MCP-1). Plate was read on the BioPlex 200 (BioRad). Concentration were extrapolated with the Bioplex Manager software (v6.1) using 5-PL curve-fitting regression algorithms with standards run in duplicate. For data representation, out of ratio values in high concentration (OOR >) were replaced with a value that is twice of the upper limit of quantification (ULOQ), which is measured in the dataset based on the standard curve. Cytokine dosage was performed at the Cytometry and Biomarker UtechS, Institut Pasteur.

Single-Molecule Array (Simoa) IFN- α Digital ELISA

Cell supernatants IFN- α concentrations were determined with Simoa technology, using reagents and procedures according to manufacturer's instructions (Quanterix SimoaTM IFN α Reagent Kit). For all supernatants, the working dilutions were 1:2, in working volumes of 170 μ L. In the first step of the assay, capture beads coated with an anti-cytokine Ab were combined with the cell

supernatants. After washing, the biotinylated detector Ab was added to the reaction to bind the captured cytokine. Following the second wash, streptavidin- β -galactosidase (SBG) was added to bind the detector Ab, resulting in enzyme labeling of the captured cytokine. After washing, the beads were resuspended in a resorufin β -D-galactopyranoside (RGP) substrate solution and immediately transferred to a Simoa disc array (Quanterix Simoa™ Disc Kit) for individual capture in the microwells. The β -galactosidase on the captured cytokine hydrolyzed the RGP substrate, yielding a fluorescent signal, for IFN α determination. The percentage of bead-containing wells in the array displaying a positive signal is proportional to the amount of cytokine present in the sample (digital measurement). Cytokine concentrations in cell supernatants were interpolated from standard curves and kit control samples.

Quantification of Gene Expression by RT-qPCR Using the BioMark HD System (Fluidigm)

RNA Preparation

All fibroblasts except the 241 cell* were seeded in 6-well culture plates at $1,4 \times 10^5$ cells/ml in a total volume of 2 ml DMEM 2% SVF. The next day, the medium was exchanged to DMEM 0,5% SVF for 48 h. Total RNA was extracted using the RNeasy Mini kit (Qiagen) which included a RNase-Free DNase treatment step to eliminate DNA contamination and RNA quality was assessed by Nanodrop spectrometry (Thermo Fisher). Reverse transcription was performed using the SuperScript II Reverse Transcriptase (Invitrogen).

*The cells of donor 241 were lost.

qRT-PCR

All sample cDNAs were first pre-amplified: a pool of TaqMan Gene Expression Assays was prepared where each 20X TaqMan Gene expression assay (human *TLR3* (Hs01551079_g1), *TLR4* (Hs00152939_m1), and control genes *HPRT1* (Hs02800695_m1), *RPL19* (Hs02338565_gH) and *TBP* (Hs00427620_m1), Thermo Fisher) is at a final concentration of 0.2X (500 nM). Target preamplification was achieved by mixing 1,25 μ l of pooled TaqMan Gene Expression Assays with 2,5 μ l PreAmp Master Mix (Fluidigm 4391128) and 1,25 μ l of each cDNA to which was applied the following cycling protocol: 95°C for 10 min, followed by 16 cycles \times (95°C for 15 s and 60°C for 4 min). The preamplification reactions were treated by Exonuclease I 4u/ μ l at 37°C for 30 min and then diluted at 1:5, 1:10 and 1:20 in Tris 10mM 0,1 mM EDTA.

For amplification, 5 μ l of each TaqMan Gene expression assay 10X in assay loading reagent (Fluidigm PN100-7611) and 5 μ l of each dilution of preamplified cDNA mixed with GE sample loading reagent (Fluidigm PN100-7610) and Taqman Fast advanced Master Mix (Life Technologies, PN4444557) were loaded on the assay and sample inlets of a 48.48 Dynamic Array™ IFC for Gene Expression (Fluidigm), after priming of the array, for use in a BioMark HD instrument.

Of the three control genes TBP, HPRT1 and RPL19, Ct values of TBP and HPRT1 (CV of 5,5% and 6,5% respectively) were the

more stable across all samples and were used to calculate the Delta Ct of the samples at dilution 1:5.

Ct values of the tested and control genes at 1:5, 1:10 and 1:20 dilutions of each sample were consistent with the dilution factor.

Statistical Analysis

Each experiment was repeated at least twice with every experimental point aggregated from triplicate sample measurement.

Mean values and standard deviation were calculated for all results.

To compare LPS high and low responders, the arithmetic means were calculated for each examined group. Comparisons between the two groups were analyzed by Mann-Whitney-U-Test. Probability values (p) were calculated and a level of $P < 0.05$ was considered as statistically significant.

Chi-square test was used for univariate analysis of percentage of cells with NF- κ B in the nucleus of the cells. Data were presented as means \pm standard deviation from at least three independent experiments. Statistical significance was defined as $P < 0.05$.

CONSORTIUM

The *Milieu Intérieur* Consortium is composed of the team leaders: Laurent Abel (Hôpital Necker), Andres Alcover, Hugues Aschard, Kalla Astrom (Lund University), Philippe Bousso, Pierre Bruhns, Ana Cumano, Caroline Demangel, Ludovic Deriano, James Di Santo, Françoise Dromer, Gérard Eberl, Jost Enninga, Jacques Fellay (EPFL, Lausanne), Ivo Gomperts-Boneca, Milena Hasan, Serge Herberg (Université Paris 13), Olivier Lantz (Institut Curie), Hugo Mouquet, Etienne Patin, Sandra Pellegrini, Stanislas Pol (Hôpital C \hat{c} ochin), Antonio Rausell (INSERM UMR 1163 – Institut Imagine), Lars Rogge, Anavaj Sakuntabhai, Olivier Schwartz, Benno Schwikowski, Spencer Shorte, Frédéric Tangy, Antoine Toubert (Hôpital Saint-Louis), Mathilde Trouvier (Université Paris 13), Marie-Noëlle Ungeheuer, Darragh Duffy[§], Matthew L. Albert (In Situ)[§], Lluís Quintana-Murci[§].

¶ unless otherwise indicated, partners are located at Institut Pasteur, Paris

[§] co-coordinators of the *Milieu Intérieur* Consortium.

Additional information can be found at <http://www.milieuinterieur.fr/>.

RESULTS

Analysis of HSV-1 Cell Infection

As a means to evaluate the variability of the innate immune response to infection of fibroblasts from different donors, we first developed an assay using HSV-1 infection using a virus engineered to express green fluorescent protein (GFP). The GFP from *Aequorea victoria* was fused with the capsid protein VP26 to generate a VP26-GFP protein expressed by the K26GFP virus. VP26 is located on the outer surface of the capsid and cells

infected with the K26GFP virus exhibited a punctate nuclear fluorescence at early times in the replication cycle. At later times during infection a generalized cytoplasmic and nuclear fluorescence, including fluorescence at the cell membranes and the spreading of infection to surrounding cells was observed (24). To our knowledge, the combination of imaging of a fluorescent signal in a high content setting to follow HSV-1 infection efficiency has not yet been described.

To evaluate the delay between HSV-1 infection and the appearance of the VP26-GFP protein in infected cells, we first performed automated imaging microscopy using the InCuCyte Zoom device (Essen Biosciences). The fluorescent signal corresponding to the production of the capsid protein-GFP (VP26), produced after a replication cycle (24), appeared only about 9–10 h after infection in our experimental conditions. This approach allowed to observe viral replication dynamics by following the fluorescent signal which appearing more rapidly indicated increased susceptibility of cells to infection (data not shown).

Our aim was to establish a robust end-point measure that would allow a quantitative assessment of the response to infection. We thus tried a large range of multiplicity of infection (from 0,004 to 10 MOI) and several incubation times after infection to determine the conditions where GFP expression was optimally detected. Based on the range of the number of infected cells detected, we chose to image the infection at 48 h post infection at between 0,01 to 0,5 MOI (data not shown).

We first followed the infection of two different cell lines (DHF and TLR3^{-/-}). According to published data, our hypothesis in developing these protocols was that the primary fibroblast cell line DHF, considered to be healthy fibroblasts, should be able to respond efficiently to HSV-1 infection due to the stimulation of the TLR3 receptor and therefore be less infected than the SV40 immortalized TLR3^{-/-} fibroblast cell line which are deficient in their TLR3 pathway, leading to increased sensitivity to infection. As shown in **Figure 1A**, the infection process can be followed through expression of GFP in the nucleus of the infected cells. Active infection of DHF cells could be detected at 48 h for an MOI of 0,01 or higher (data not shown). Image analysis performed as described in Materials and Methods, showed that at 0,1 MOI, 80–90% of DHF cells are infected versus only 40–50% for TLR3^{-/-} cells. At 0,5 MOI 90 to 95% of DHF and TLR3^{-/-} cells are infected (**Figure 1B**). Thus, unexpectedly TLR3^{-/-} cells appeared to be less sensitive than DHF cells at a 0,1 MOI infection by HSV-1 and to have comparable sensitivity at 0,5 MOI. By way of positive control, we also verified that treatment with interferon α -2b (10⁵ UI/ml) prior to infection totally protected the cells (data not shown).

We then analyzed a series of immortalized fibroblasts from patients carrying mutations in the TLR3 pathway and control cells that impact susceptibility to HSV-1 infection, as described by J-L. Casanova and collaborators (18–20).

Unexpectedly, we observed that immortalized C65 and C72 human fibroblasts from healthy donors are less sensitive to HSV-1 infection compared to a primary fibroblast DHF (10–15% compared

to 90–95% at a 0,5 MOI), which may indicate that immortalization would confer resistance to HSV-1 infection (**Figure 1B**). Moreover, two other widely used non-immortalized healthy fibroblast cell lines, WI-38 and BJ, have a susceptibility to HSV-1 infection similar to that of TLR3^{-/-} cells (**Figure S1**).

Mutant cells for TLR3^{+/-} (2018), TRIF, TLR3^{+/-} (1323), Nemo, TBK1 and TLR3^{-/-} showed a higher susceptibility to infection than the immortalized fibroblasts from healthy donors (C65 & C72) with respectively 25%, 35%, 50%, 60%, 60% and 90% of infected cells, compared to 10–15% for healthy controls C65 and C72 cells, at 0.5 MOI (**Figure 1B**).

Stimulation of Cells by Poly I:C

As for the *LabEx* MI whole blood study (2), we searched for stimulation conditions providing defined molecular stimuli of innate immune responses with viral or bacterial MAMPs. Based on published data (19, 29) on poly I:C stimulation of fibroblasts, we tried the concentrations ranging from 10 to 100 μ g/ml for 22 h incubation time using in parallel, primary and immortalized fibroblasts. Immortalized fibroblasts with mutations of the TLR3 pathway were also used in order to better evaluate the range of sensitivity for our read-out of cell activation, the percentage of cells having translocated NF- κ B to the nucleus.

We next determined the conditions for optimal activation of the primary fibroblasts DHF by poly I:C in comparison with TLR3^{-/-} cells. TLR3^{-/-} cells displayed no response to poly I:C stimulation (10 μ g/ml) whereas DHFs cells were activated (**Figure 1C**), 60%–70% of the cells showing a nuclear NF- κ B signal (**Figure 1D**). The immortalized C65 and C72 fibroblasts from healthy individuals were used as controls for the mutant cells. As shown in **Figure 1D**, the C65, C72 and DHFs cells were maximally activated (70–90%) at a concentration of 5 μ g/ml to 10 μ g/ml poly I:C, the highest concentration evoking responses in around 80–90% of cells. Under the same conditions TLR3 mutant cell lines were generally less activated by poly I:C. The NF- κ B protein was very little or not at all translocated in the nuclei of the cells carrying mutation in the Nemo or TRIF proteins (5%–25%) and the NF- κ B translocation was only observed in 30%–40% of the cells carrying TBK1 mutation. Consistent with their genotype TLR3^{-/-} double mutant cells did not respond at all to poly I:C and 1323 and 2018 both heterozygous for TLR3 mutation (TLR3^{+/-}) showed a low response (15% and 40%, respectively; **Figure 1D**).

Variability of the Response of LabEx MI Primary Fibroblasts to Poly I:C and Lipopolysaccharide

We then studied the response to poly I:C and LPS stimulation of a series of 13 primary fibroblasts from the *LabEx* MI using the “Add-only” protocol. As for poly I:C, we first evaluated the effect of different concentrations of LPS and incubation time on the activation of the cells defined as cells having translocated NF- κ B from the cytoplasm to the nucleus. The incubation time was in the range of 1 to 3 h, the highest signal following 3 h incubation.

Using LPS concentrations ranging from 10 to 100 ng, we observed that the number of responding cells increased with the

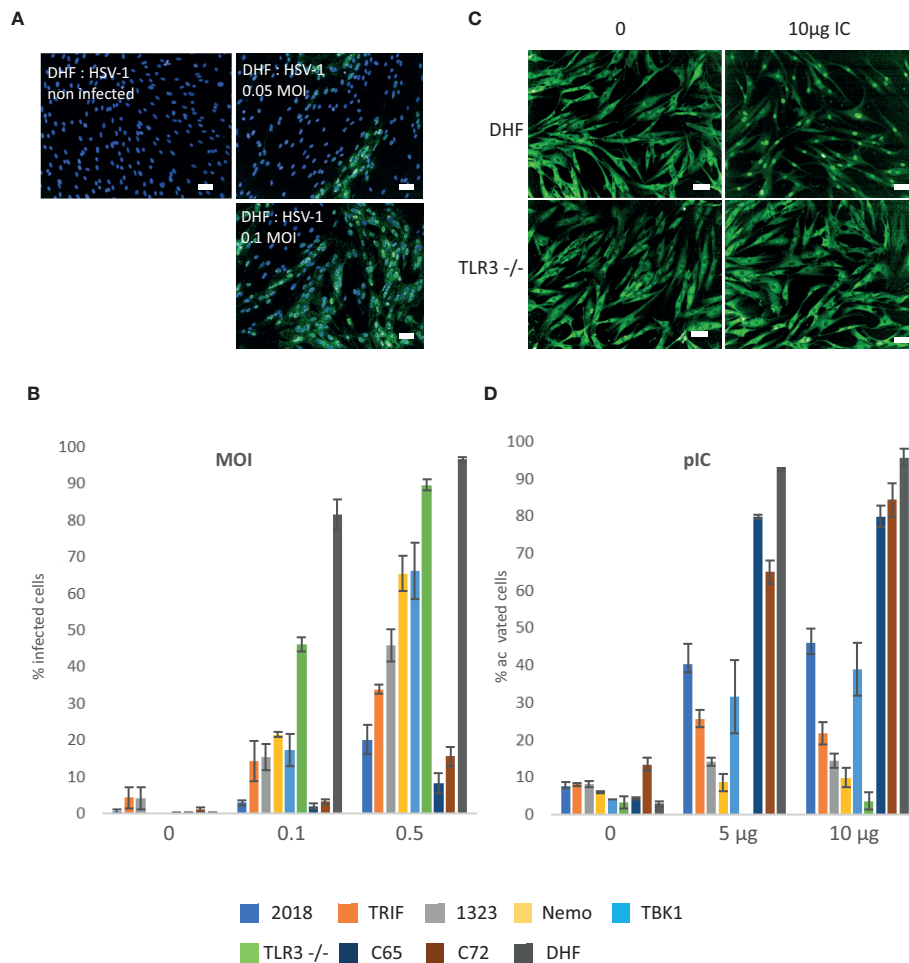


FIGURE 1 | HSV1- green fluorescent protein (GFP) infection and response to Poly (I:C) stimulation of healthy and mutant fibroblasts. **(A, B)** HSV1-GFP infection of healthy and mutant fibroblasts **(A)** Overlays of the detection of the fluorescence signal in DHF cells (green) infected at 0.05, 0.1 MOI and non-infected controls with a nuclei Hoechst counterstain (blue). Images were acquired on an Opera QEH5 system with a 10x objective and correspond to one field of view. Scale bar: 50µm. **(B)** Quantification of the percentage of infected cells after infection with 0, 0.1 and 0.5 MOIs. Compiled results of the mean percentages presented together for comparison: 2018 (TLR3 +/- cells), Trif (TRIF-/- cells), 1323 (TLR3 +/- cells), Nemo (NEMO -/- cells), TBK1 (TBK1 -/- cells), TLR3-/- cells, control cells C65 et C72, and DHF. Bars plot the mean \pm sd of triplicates of each experimental point. All cell lines are SV40 immortalized fibroblasts except DHF which are primary fibroblasts. **(C, D)** Poly (I:C) stimulation of healthy and mutant fibroblasts **(C)** Representative images of the immunofluorescence signal of DHF (upper part) and TLR3-/- (lower part) fibroblasts labeled with an anti- NF- κ B antibody: non-stimulated cells (left) and stimulated with 10µg Poly (I:C). Scale bar: 50µm. **(D)** Percentage of cells with nuclear NF- κ B (activated) for cells stimulated with 1µg and 10µg of Poly (I:C) and control unstimulated cells (0): 2018 (TLR3 +/- cells), Trif (TRIF-/- cells), 1323 (TLR3 +/- cells), Nemo (NEMO -/- cells), TBK1 (TBK1 -/- cells), TLR3-/- cells, control cells c65 et c72, and DHF. Bars plot the mean \pm sd of triplicates of each experimental point. All cell lines are SV40 immortalized fibroblasts except DHF which are primary fibroblasts.

concentration and reached a maximum of 80%–90% activated cells for some of the donors at a concentration of 100 ng/ml. Other cells were activated in the range of 30 to 50% and one donor fibroblast sample (323) showed no response at all. The **Figure 2A** presents the combined mean and standard deviation measured from different experiments represented together for the comparison.

We evaluated the robustness of the LPS cellular responses to be preserved characteristically by measuring the reproducibility over time of the cell response in two cell samples. The same experiment was performed with two donor samples (209 and 818) at an 18 month interval. In the first experiment, 209 and 818

cells were both at passage 8. In the second experiment, 209 cells were at passage 14 and 818 cells at passage 11 (**Figure 2B**). The relatedness of the two experimental results was evaluated by a χ^2 test. There was no significant difference at a p-value superior to 0.05. Thus, the results were essentially the same.

We next assessed the response of the non-responder (323), a “low” responder (318) and two “high” responder (818 and 820) donor samples, as defined from the percentage of cells with nucleus NF- κ B after LPS stimulation, to the stimulation by LPS (**Figure 3A**), poly I:C (**Figure 3B**) and TNF α (data not shown). All the cells were very similar in their responses to poly I:C and TNF α (data not shown), the response to poly I:C being a little

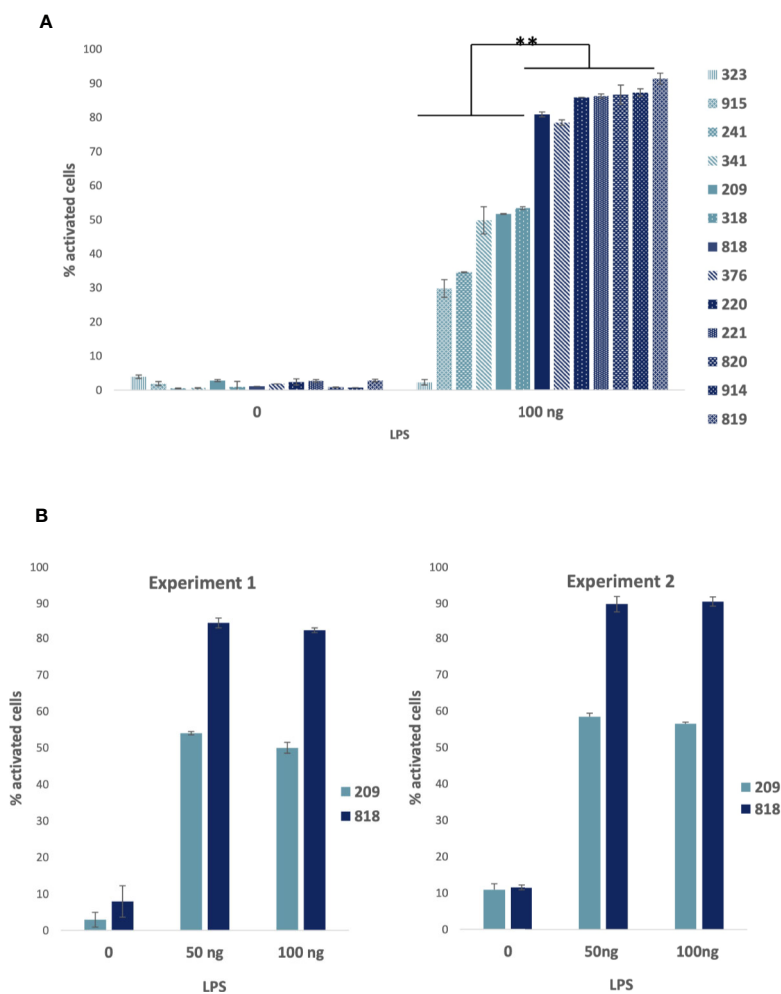


FIGURE 2 | Lipopolysaccharide (LPS) stimulation of healthy fibroblasts. **(A)** LPS stimulation of 13 primary fibroblasts from the *LabEx Milieu interieur* collection: Percentage of cells with nuclear NF- κ B (activated): compiled results of average percentages presented together for comparison of cells stimulated with 100 ng LPS for 3 h and controls. Bars plot the mean \pm sd of triplicates of each experimental point. 209, 220, 221, 241, correspond to women age 30–39; 318, 323, 341, 376 to men age 30–39; 818, 819, 820 to women age 60–69; and 914, 915: men age 60–69. Low responders are shown in light blue and high responders in dark blue. Statistical analyses were carried out using the Mann–Whitney–U-Test and p values < 0.05 were considered as statistically significant. ** Significant differences between low and high responders. **(B)** Percentage of cells with nuclear NF- κ B (activated) for donors' fibroblasts (women: 209, age 30–39 and 818, age 60–69) activated with 50 and 100 ng of LPS or non-stimulated (0): results of two experiments performed at one year and a half apart. Bars plot the mean \pm sd of triplicates of each experimental point. Chi-square test analysis of the results showed that differences between the two experiments were statistically not significant at a p value < 0.05 .

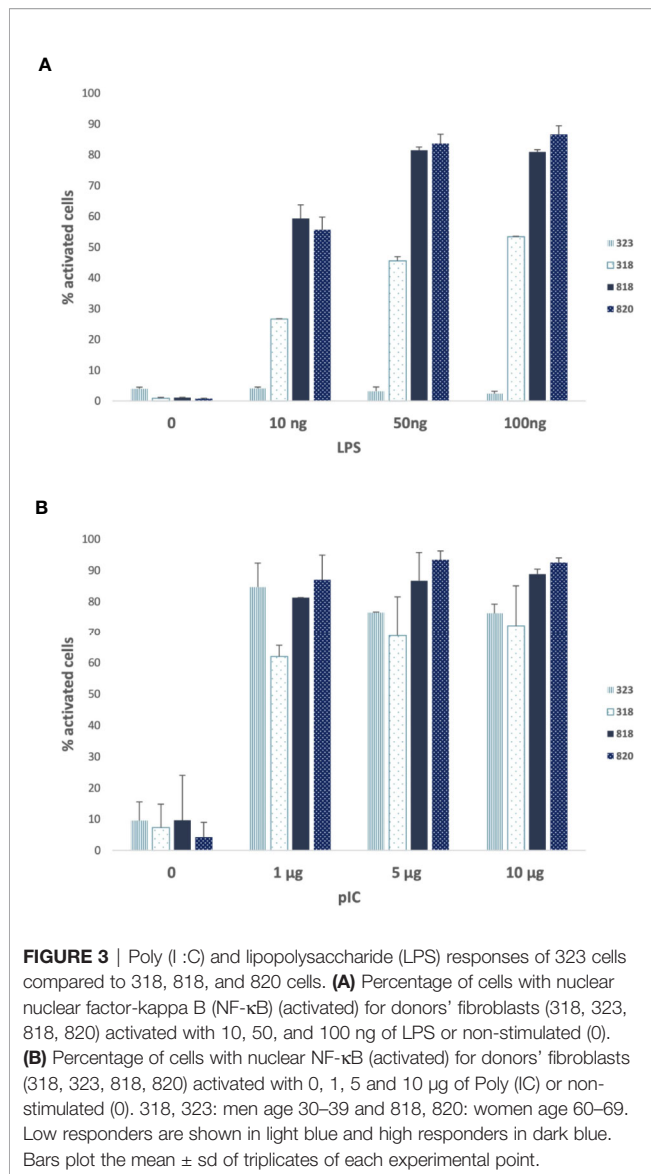
less pronounced for 323 and 318 compared to the two other cells. Therefore, the deficient response of 323 cells appeared to be specific to the MyD88 arm of the TLR4 pathway.

We also evaluated the effect of the number of passages of primary fibroblasts on their response to stimulation. Indeed, it was generally accepted that fibroblasts must be analyzed before passage 10 at the latest and that it was preferable to compare the behavior of cells studied with equivalent passages.

We repeated the same experiment with cells at different passages. We observed that the response of the cells was not affected by the number of passages between 4 and 9 for poly I:C concentrations of 5 to 20 μ g/ml (data not shown) and 8 to 14 as already shown for LPS stimulation (**Figure 2B**).

Flow Cytometry and Cytokine dosage of Poly I: C and Lipopolysaccharide Stimulated Fibroblasts

When comparing the response of the cells to various stimulations, we observed that the responses to LPS stimulation were distributed between “low” responder and “high” responders, while the inter-donor variability in the response to poly I:C was very low and the response to TNF α always involved 100% of the cells. To better evaluate the biological significance of the information consisting in the number of cells with NF- κ B in the nucleus after stimulation, we stimulated fibroblasts from donor 209 (a LPS “low” responder), and donor 818, (a LPS “high” responder), with LPS and poly I:C measuring IL-6 and IL-8 in the cell culture supernatants. The



expression of IL-6 was much strongly augmented in LPS stimulated cells from donor 818, but not cells from donor 209; whereas IL-8 was stimulated in both donors' fibroblasts stimulated by LPS, but significantly more in cells from donor 818 than in donor 209. By contrast, stimulation by poly I:C induced a similar augmentation of both cytokines in the cell culture supernatants from both donors 209 and 818 (**Figure 4A**).

In parallel we analyzed the cellular expression levels of IL-6 and IL-8 in LPS and poly I:C stimulated samples prepared from donors 209 and 818 using single cell flow cytometry analysis. We observed that there were fewer cells expressing IL-6 and IL-8 cytokines in the LPS stimulated LPS “low responder” fibroblasts (donor 209) than in the LPS “high responder” (donor 818) (5% versus 39% for IL-6 and 20.7% versus 47.7% for IL-8, **Figure 4B**, left). By contrast, there was little difference between the responses of the two populations of fibroblasts stimulated by poly I:C (26.5% versus 23.1% for IL-6 and 45.4% versus 43% for IL-8,

Figure 4B, right). Thus fibroblasts prepared from the donors 209 and 818 followed the same LPS and poly I:C response trend in both single cell cytokine expression, and cytokines released into the supernatant (**Figure 4**).

Two other cytokines were analyzed in the same supernatants. Cytokine CCL2 (MCP-1) followed the same trend as IL-6 and IL-8 in the supernatants of 209 and 818 cells (**Figure 4A**). However, Luminex data of IFN α were not interpretable. We thus used the Simoa (single-molecule array digital ELISA) which enables the direct quantification of IFN α at attomolar (femtograms per milliliter) concentrations (30). A similar concentrations of IFN α at about 2,6 pg/ml was detected in every cell and culture conditions supernatants, a concentration equivalent to one of the kit controls (**Figure S2**).

Expression of TLR3 and TLR4 Genes in “High” and “Low” Responder Cells

We observed that responses to LPS stimulation were distributed between “low” and “high” responders, while the inter-donor variability of the response to poly I:C was very low. Poly I:C and LPS stimulate activation pathways from TLR3 and TLR4 receptors, respectively. A first hypothesis to explain the variability of the responses of primary fibroblasts to LPS would be that the cells of “low” responders express fewer TLR4 receptors than cells of “high” responders while the levels of TLR3 expression should be more uniform between cells.

We therefore set up a real-time quantitative PCR assay of the twelve cells in parallel using the BioMark automated PCR system (Fluidigm) for comparative quantification of TLR3 and TLR4 mRNAs in the donors' fibroblasts. Gene expression profile were evaluated comparing the Delta Ct values between all cells using HPRT1 or TBP as reference gene (**Figures 5A, B**, respectively). Contrary to our hypothesis there is little difference in baseline TLR3 and TLR4 expression level between cells, and in particular no difference in baseline TLR4 expression level between “high” and “low” LPS responder cells. In addition, no TLR4 mRNA was detected in 323 cells (data not shown).

DISCUSSION

In this study, we report methods and protocol validating the proof-of-concept for quantitative cell-based assays useful to evaluate biologically relevant innate immune response in primary fibroblasts.

First, we used imaging of a fluorescent signal in a high content setting to follow HSV-1 infection efficiency. The assay is applicable to medium to high-throughput screening for anti-viral compounds as well as basic studies of cellular antiviral signaling. The observed responses were consistent with the data published for these mutants of the TLR3 pathway to HSV-1 infection (18, 19, 26, 29). Using this same protocol, we also observed that primary and immortalized human fibroblasts from healthy donors had different susceptibilities to HSV-1 infection. The fibroblasts used in our experiments were immortalized using the expression of the virus SV40 Large T (LT) antigen. SV40 LT interacts with endogenous proteins of the cells to induce immortalization, notably with the retinoblastoma protein, Rb, and with p53. In epithelial cells it was shown that Rb with E2F1

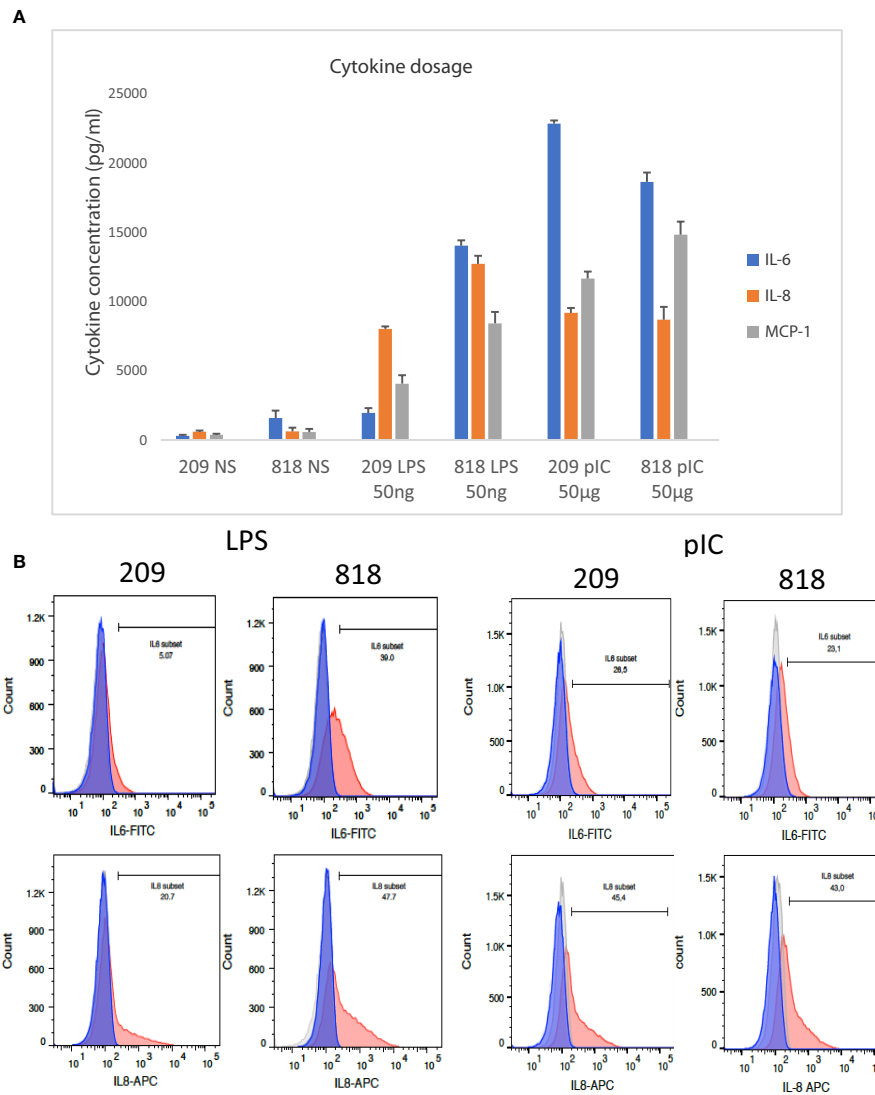


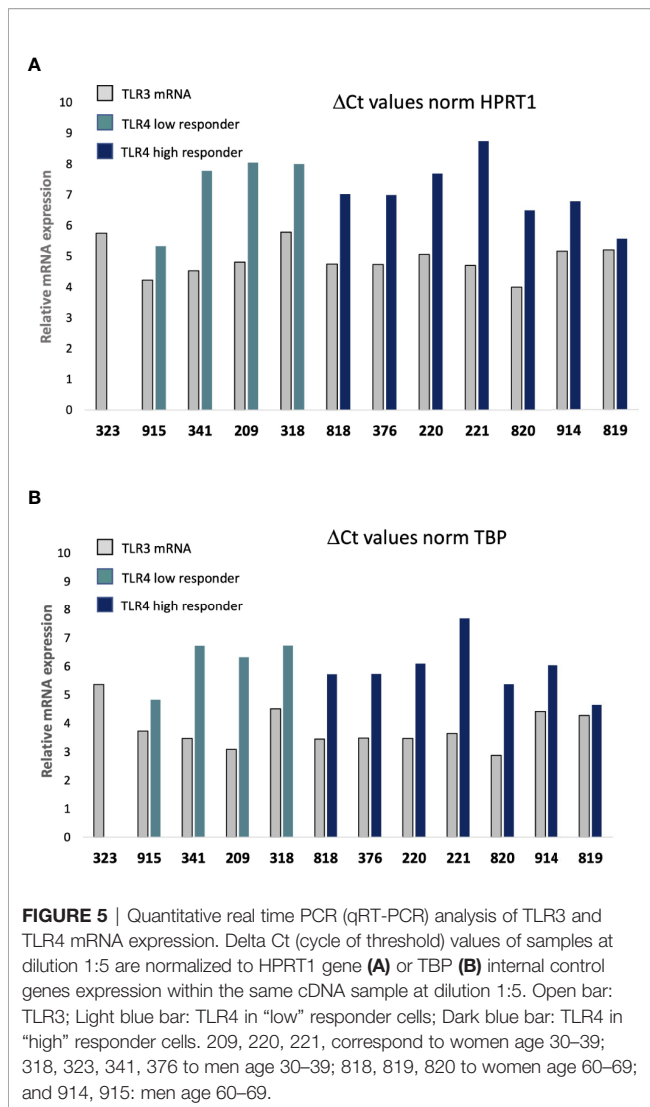
FIGURE 4 | Analysis of cytokine expression by FACS and Luminex dosage. **(A)** IL-6, IL-8, and CCL2 cytokine dosage in the supernatant of 209 and 818 stimulated by lipopolysaccharide (LPS) and poly (I:C) and non-stimulated controls. Bars plot the mean \pm sd of triplicates of each experimental point. Concentrations are given in pg/ml. **(B)** Flow cytometry analysis of IL-6 and IL-8 expressed by fibroblasts after LPS or poly (I:C) stimulation and control non-stimulated cells: the light grey histogram corresponds to non-labeled non-stimulated cells, the dark grey to stimulated non-labeled cells, the blue histogram represents non stimulated labeled cells and the red histogram cells stimulated and labeled. The bar indicates the percentage of labeled cells in stimulated conditions compared to controls. On the left: comparison of 209 and 818 cells stimulated by LPS; on the right: comparison of 209 and 818 cells stimulated by poly (I:C).

and p53 regulates the innate immune receptor TLR3 (31, 32). In addition, immune response genes including interferon-stimulated genes are upregulated in cells expressing SV40 LT (33). This upregulated innate immune response may therefore explain the lower sensitivity of immortalized cells to HSV-1 infection, particularly at low MOI. These observations emphasize the importance of working with primary cells in place of SV40 LT immortalized cells to study the response to immune stimulants.

We developed an “add-only” protocol for stimulating cells by MAMPs and cytokines that minimized sample manipulation (no washing steps) that can give rise to well-to-well variability. This protocol was applied to three different cell types, primary fibroblasts,

commercial lines and immortalized fibroblasts carrying mutations of the TLR3 pathway and allowed to differentiate individual responses based on the agonist concentration to which the cells respond. Inasmuch as cells displaying a low response level to poly I:C appeared to be inversely highly responsive to HSV-1 infection, both assays allowed to rank the innate immune response involving the TLR3 pathway of SV40-immortalized cells from patients with deficiencies in this pathway. Whether this would apply to primary fibroblasts is not clear as only a low-range variability was observed in the response to poly I:C in primary cells.

Of particular interest to us, we have measured the significant inter-individual variability of the response to innate immune



stimuli in primary fibroblasts of the MI collection (percentage of cells activated by nuclear NF- κ B). Such interindividual variability has mainly been observed in the response to LPS stimulation, allowing to define “low” and “high” responses, whereas responses to TNF or to poly IC displayed no or low level variability. These different responses to poly I:C, LPS or TNF α probably reflect the efficiency of the pathways elicited by the corresponding receptors on NF- κ B activation. This must happen downstream of the receptors, as baseline expression of TLR3 and TLR4 varies little from cell to cell, especially TLR4 expression between “high” and “low” LPS responder cells.

No differences related to age or gender were observed among the 13 MI-cohort donors. High responses in the older donors could be a consequence of cell aging, a phenomenon called inflammaging (34), however high responses are also observed in cells from younger donors. The observed responses are robust as we obtained essentially the same results for LPS stimulation of two cells (209 and 818) performed at an interval of eighteen months. Altogether, these results demonstrate that the “add-only” protocol actually

allows to describe the interindividual variability of the innate immune response of human primary fibroblasts in culture. In addition, the cells of one donor (323) out of 13, did not respond to LPS, but were stimulated by poly I:C and TNF α . Although we had verified that this donor carried no SNPs in the TLR4 that were described to alter the response to LPS stimulation (35, 36), no TLR4 mRNA was detected by qRT-PCR analysis in 323 cells. This observation fully explains the absence of response to LPS of these cells. However, the 323 cells were from a healthy donor with a medium level blood cell response to LPS and normal baseline expression of TLR4 transcripts in blood cells (data not shown). Future research will focus on the expression of TLR4 in 323 cells upon innate immune stimulation and if TLR4 is still not expressed, the structure of the TLR4 gene in 323 cells will be studied.

Finally, these high and low responses in fibroblasts do not correspond to high and low responses to LPS in the blood of the same donor (data not shown) which is consistent with previous observations (37).

This is to our knowledge the first description of interindividual variability of the response of human primary fibroblast from healthy donors to innate immune stimulation. Individuals who consistently produced high or low concentrations of cytokines (most notably IL-1 β , IL-6, IL-8, and TNF- α) in whole-blood samples after LPS stimulation had been previously identified. These phenotypes were stable, and corresponded to significant gene expression differences (38).

Similarly to our results, analysis of the variability of cattle dermal fibroblasts responses to LPS allowed *low responder* (LR) and *high responder* (HR) classification (39) for IL-6 and IL-8 cytokines secretion. The expression of many TLR-regulated genes, such as IL-6 and IL-8, were several-fold less in the LR compared to HR fibroblasts after LPS stimulation. Accordingly, levels of IL-6 and IL-8 were higher in HR compared to LR fibroblasts after LPS stimulation (39). These results suggest that the amplitude of the cells’ response to immunity stimulants may rely on a pre-existing arrangement of molecular networks that would dictate the characteristics of this response, quantitatively and possibly qualitatively.

We hypothesize that the different percentages of cells with nuclear NF- κ B after LPS stimulation reflect a similar variability of fibroblasts’ response *in vivo* reflecting donor immune-status relevant information. We analyzed the expression of IL-6 and IL-8 by LPS, or poly I:C stimulated fibroblasts from donors 209 and 818 detecting secreted (supernatant), and in parallel single-cell expression by flow cytometry. Interestingly, we have observed that there were fewer cells expressing cytokines in “low responder” fibroblasts (209) than in “high responder” (818) fibroblasts for LPS stimulation. On the other hand, there was no significant difference between the responses of these same two populations of fibroblasts stimulated by poly I: C. Levels of IL-6 and IL-8 in the supernatants and populations of IL-6 and IL-8 expressing cells were consistent with the percentage of activated cells defined by the presence of NF- κ B in the nucleus, suggesting the biological significance of this read-out. Levels of CCL2 in the supernatants followed the same trend as IL-6 and IL-8 whereas levels of INF α remained unchanged.

Direct measurement of type I IFN protein in biological samples has remained elusive until the development of the

SIMOA technology as described in Rodero et al. (30). Consequently, to the best of our knowledge, there is no published data on INF α concentration in the supernatants of fibroblast cell cultures. It was recently proposed that secreted INF α is immediately bound by its receptors and internalized and then persists in endosomal compartments, termed IFN silos (40).

Altogether, our observations suggest that fibroblasts from different donors display inter-individual variable responses to innate immune stimuli, that may translate into a stromal-specific inter-individual response variability. Indeed, stromal specific regulation of the IL-6 pathway have already been presented (9, 10). Fibroblasts are a major component of the stroma where they can be exposed to microbes as well as to DAMPs in sterile inflammation and cancer. The contribution of human non-professional, tissue resident cells to protective immunity to infection were recently described (41). There is no description of fibroblasts among these non-professional cells, although the role of fibroblasts in the defense against pathogens has already been documented (12). Higher or lower responses to innate immune stimulants, together with a yet to be described putative qualitative variability of these responses, would probably impact the role of fibroblasts in tissue homeostasis and their dialog with immune cells (42).

Our next steps will consider assessing the secretion level of a larger number of cytokines under these same conditions in order to better characterize the variability of this response quantitatively and qualitatively. Altogether we propose robust protocols that unravel the variability of the primary fibroblasts' responses based on the detection of the p65/NF- κ B or imaging GFP-tagged VP26 (HSV-1). These protocols are new tools to better evaluate the functional responses of fibroblasts to a wide range of immune stimulants and their variability, a biological immune-response tissue niche whose importance has only recently come to be recognized. Indeed, subsets of fibroblasts are now directly implicated in the pathogenesis of diseases including cancer, myocardial infarction and chronic lung disease in addition to fibrotic diseases classically associated with fibroblasts.

DATA AVAILABILITY STATEMENT

The original contributions presented in the study are included in the article/**Supplementary Material**. Further inquiries can be directed to the corresponding authors.

ETHICS STATEMENT

The studies involving human participants were reviewed and approved by Comité de protection des personnes – Ouest 6 (Committee for the protection of persons) on June 13, 2012 and French Agence nationale de sécurité du médicament (ANSM) on June 22, 2012. The patients/participants provided their written informed consent to participate in this study.

CONSORTIUM

The Milieu Intérieur Consortium is composed of the team leaders: Laurent Abel (Hôpital Necker), Andres Alcover,

Hugues Aschard, Kalla Astrom (Lund University), Philippe Bouso, Pierre Bruhns, Ana Cumano, Caroline Demangel, Ludovic Deriano, James Di Santo, Françoise Dromer, Gérard Eberl, Jost Enninga, Jacques Fellay (EPFL, Lausanne), Ivo Gomperts-Boneca, Milena Hasan, Serge Hercberg (Université Paris 13), Olivier Lantz (Institut Curie), Hugo Mouquet, Etienne Patin, Sandra Pellegrini, Stanislas Pol (Hôpital C \hat{c} ochin), Antonio Rausell (INSERM UMR 1163 – Institut Imagine), Lars Rogge, Anavaj Sakuntabhai, Olivier Schwartz, Benno Schwikowski, Spencer Shorte, Frédéric Tangy, Antoine Toubert (Hôpital Saint-Louis), Mathilde Trouvier (Université Paris 13), Marie-Noëlle Ungeheuer, Darragh Duffy[§], Matthew L. Albert (In Situ)[§], Lluís Quintana-Murci[§].

[¶] unless otherwise indicated, partners are located at Institut Pasteur, Paris.

[§] co-coordinators of the Milieu Intérieur Consortium.

Additional information can be found at <http://www.milieuinterieur.fr/>

AUTHOR CONTRIBUTIONS

AC, MM, ND, PF, TS, MH, NA, BD-W conducted the experiments and analysis. LabExMI and GZ provided the resources. SLS and BD-W conceptualized the study. BD-W designed the study, collected the data, and wrote the manuscript. All authors contributed to the article and approved the submitted version.

FUNDING

We are grateful for support from the French Government Agence nationale de la recherche (ANR) programmes: Investissements d'Avenir programme ('Laboratoire d'Excellence Integrative Biology of Emerging Infectious Diseases'; grant ANR-10-LABX-62-IBEID, "Laboratoire Revive"; grant ANR 10-LBX-73-REVIVE, "Laboratoire d'Excellence Milieu interieur"; grant ANR-10-LABX-69-01); France BioImaging (FBI; grant ANR-10-INSB-04-01), the Région Ile de France (Domaine d'intérêt majeur One Health, DIMIHealth) and the GIS IBISA (Infrastructures en biologie santé et agronomie), and the Institut Pasteur.

ACKNOWLEDGMENTS

The authors thank Catherine Werts and Jong Eun Ihm for critical reading of the manuscript. BDW also thanks the members of the UTechS Photonic BioImaging (PBI) and UTechS Cytometry and Biomarkers (CB) of the Institut Pasteur for their support, and E. Karkeni, F. Vernel-Pauillac and D. Bonhomme for technical help and advices.

SUPPLEMENTARY MATERIAL

The Supplementary Material for this article can be found online at: <https://www.frontiersin.org/articles/10.3389/fimmu.2020.569331/full#supplementary-material>

REFERENCES

- Thomas S, Rouilly V, Patin E, Alanio C, Dubois A, Delval C, et al. The Milieu Intérieur study - an integrative approach for study of human immunological variance. *Clin Immunol* (2015) 157(2):277–93. doi: 10.1016/j.clim.2014.12.004
- Duffy D, Rouilly V, Libri V, Hasan M, Beitz B, David M, et al. Functional analysis via standardized whole-blood stimulation systems defines the boundaries of a healthy immune response to complex stimuli. *Immunity* (2014) 40(3):436–50. doi: 10.1016/j.immuni.2014.03.002
- Urrutia A, Duffy D, Rouilly V, Posseme C, Djebali R, Illanes G, et al. Standardized Whole-Blood Transcriptional Profiling Enables the Deconvolution of Complex Induced Immune Responses. *Cell Rep* (2016) 16(10):2777–91. doi: 10.1016/j.celrep.2016.08.011
- Piasecka B, Duffy D, Urrutia A, Quach H, Patin E, Posseme C, et al. Distinctive roles of age, sex, and genetics in shaping transcriptional variation of human immune responses to microbial challenges. *Proc Natl Acad Sci U S A* (2018) 115(3):E488–97. doi: 10.1073/pnas.1714765115
- Sorrell JM, Caplan AI. Fibroblasts—a diverse population at the center of it all. *Int Rev Cell Mol Biol* (2009) 276:161–214. doi: 10.1016/S1937-6448(09)76004-6
- Tabeta K, Yamazaki K, Akashi S, Miyake K, Kumada H, Umemoto T, et al. Toll-like receptors confer responsiveness to lipopolysaccharide from *Porphyrromonas gingivalis* in human gingival fibroblasts. *Infect Immun* (2000) 68(6):3731–5. doi: 10.1128/iai.68.6.3731-3735.2000
- Kawai T, Akira S. TLR signaling. *Semin Immunol* (2007) 19(1):24–32. doi: 10.1016/j.smim.2006.12.004
- Schaefer L. Complexity of danger: the diverse nature of damage-associated molecular patterns. *J Biol Chem* (2014) 289(51):35237–45. doi: 10.1074/jbc.R114.619304
- Noss EH, Nguyen HN, Chang SK, Watts GF, Brenner MB. Genetic polymorphism directs IL-6 expression in fibroblasts but not selected other cell types. *Proc Natl Acad Sci U S A* (2015) 112(48):14948–53. doi: 10.1073/pnas.1520861112
- Nguyen HN, Noss EH, Mizoguchi F, Huppertz C, Wei KS, Watts GFM, et al. Autocrine Loop Involving IL-6 Family Member LIF, LIF Receptor, and STAT4 Drives Sustained Fibroblast Production of Inflammatory Mediators. *Immunity* (2017) 46(2):220–32. doi: 10.1016/j.immuni.2017.01.004
- Jolly AL, Rau S, Chadha AK, Abdurraheem EA, Dean D. Stromal fibroblasts drive host inflammatory responses that are dependent on Chlamydia trachomatis strain type and likely influence disease outcomes. *mBio* (2019) 10(2):e00225–19. doi: 10.1128/mBio.00225-19
- Kühbacher A, Henkel H, Stevens P, Grumaz C, Finkelmeier D, Burger-Kentischer A, et al. Central Role for Dermal Fibroblasts in Skin Model Protection against *Candida albicans*. *J Infect Dis* (2017) 215(11):1742–52. doi: 10.1093/infdis/jix153
- Salzer ACD, David SA. Transcriptomal signatures of vaccine adjuvants and accessory immunostimulation of sentinel cells by toll-like receptor 2/6 agonists. *Hum Vaccin Immunother* (2018) 14(7):1686–96. doi: 10.1080/21645515.2018.1480284
- LeBleu VS, Neilson EG. Origin and functional heterogeneity of fibroblasts. *FASEB J* (2020) 34(3):3519–36. doi: 10.1096/fj.201903188R
- Kim-Hellmuth S, Bechheim M, Pütz B, Mohammadi P, Nédélec Y, Giangreco N, et al. Genetic regulatory effects modified by immune activation contribute to autoimmune disease associations. *Nat Commun* (2017) 8(1):266. doi: 10.1038/s41467-017-00366-1
- Wang J, Hori K, Ding J, Huang Y, Kwan P, Ladak A, et al. Toll-like receptors expressed by dermal fibroblasts contribute to hypertrophic scarring. *J Cell Physiol* (2011) 226(5):1265–73. doi: 10.1002/jcp.22454
- Yao C, Oh JH, Lee DH, Bae JS, Jin CL, Park CH, et al. Toll-like receptor family members in skin fibroblasts are functional and have a higher expression compared to skin keratinocytes. *Int J Mol Med* (2015) 35(5):1443–50. doi: 10.3892/ijmm.2015.2146
- Sancho-Shimizu V, Pérez de Diego R, Lorenzo L, Halwani R, Alangari A, Israelson E, et al. Herpes simplex encephalitis in children with autosomal recessive and dominant TRIF deficiency. *J Clin Invest* (2011) 121(12):4889–902. doi: 10.1172/JCI59259
- Guo Y, Audry M, Ciancanelli M, Alsina L, Azevedo J, Herman M, et al. Herpes simplex virus encephalitis in a patient with complete TLR3 deficiency: TLR3 is otherwise redundant in protective immunity. *J Exp Med* (2011) 208(10):2083–98. doi: 10.1084/jem.20101568
- Zhang SY, Jouanguy E, Ugolini S, Smahi A, Elain G, Romero P, et al. TLR3 deficiency in patients with herpes simplex encephalitis. *Science* (2007) 317(5844):1522–7. doi: 10.1126/science.1139522
- De Chiara G, Marocchi ME, Sgarbanti R, Civitelli L, Ripoli C, Piacentini R, et al. Infectious agents and neurodegeneration. *Mol Neurobiol* (2012) 46(3):614–38. doi: 10.1007/s12035-012-8320-7
- Looker KJ, Magaret AS, May MT, Turner KME, Vickerman P, Gottlieb SL, et al. Global and Regional Estimates of Prevalent and Incident Herpes Simplex Virus Type 1 Infections in 2012. *PLoS One* (2015) 10(10):e0140765. doi: 10.1016/S2214-109X(16)30362-X
- Melchjorsen J. Sensing herpes: more than toll. *Rev Med Virol* (2012) 22(2):106–21. doi: 10.1002/rmv.716
- Desai P, Person S. Incorporation of the green fluorescent protein into the herpes simplex virus type 1 capsid. *J Virol* (1998) 72(9):7563–8. doi: 10.1128/JVI.72.9.7563-7568.1998
- Boisson B, Laplantine E, Prando C, Giliani S, Israelsson E, Xu Z. Immunodeficiency, autoinflammation and amylopectinosis in humans with inherited HOIL-1 and LUBAC deficiency. *Nat Immunol* (2012) 12(11):1178–86. doi: 10.1084/jem.20141130
- Herman M, Ciancanelli M, Ou YH, Lorenzo L, Klauedel-Dreszler M, Pauwels E, et al. Heterozygous TBK1 mutations impair TLR3 immunity and underlie herpes simplex encephalitis of childhood. *J Exp Med* (2012) 209(9):1567–82. doi: 10.1084/jem.20111316
- Smahi A, Courtois G, Vabres P, Yamaoka S, Heuertz S, Munnich A, et al. Genomic rearrangement in NEMO impairs NF- κ B activation and is a cause of incontinentia pigmenti. *Nature* (2000) 405(6785):466–72. doi: 10.1038/35013114
- Le Guezennec X, Quah J, Tong L, Kim N. Human tear analysis with miniaturized multiplex cytokine assay on “wall-less” 96-well plate. *Mol Vis* (2015) 21:1151–61.
- Audry M, Ciancanelli M, Yang K, Cobat A, Chang HH, Sancho-Shimizu V, et al. NEMO is a key component of NF- κ B- and IRF-3-dependent TLR3-mediated immunity to herpes simplex virus. *J Allergy Clin Immunol* (2011) 128(3):610–7.e1–4. doi: 10.1016/j.jaci.2011.04.059
- Rodero MP, Decalf JV, Bondet V, Hunt DD, Rice GI, Werneke S, et al. Detection of interferon alpha protein reveals differential levels and cellular sources in disease. *J Exp Med* (2017) 214(5):1547–55. doi: 10.1084/jem.20161451
- Taura M, Eguma A, Suico MA, Shuto T, Koga T, Komatsu K, et al. p53 regulates Toll-like receptor 3 expression and function in human epithelial cell lines. *Mol Cell Biol* (2008) 28(21):6557–67. doi: 10.1128/MCB.01202-08
- Taura M, Suico MA, Koyama K, Komatsu K, Miyakita R, Matsumoto C, et al. Rb/E2F1 regulates the innate immune receptor Toll-like receptor 3 in epithelial cells. *Mol Cell Biol* (2012) 32(8):1581–90. doi: 10.1128/MCB.06454-11
- Rathi AV, Cantalupo PG, Sarkar SN, Pipas JM. Induction of interferon-stimulated genes by Simian virus 40 T antigens. *Virology* (2010) 406(2):202–11. doi: 10.1016/j.virol.2010.07.018
- Freund A, Orjalo AV, Desprez PY, Campisi J. Inflammatory networks during cellular senescence: causes and consequences. *Trends Mol Med* (2010) 16(5):238–46. doi: 10.1016/j.molmed.2010.03.003
- Figueroa L, Xiong Y, Song C, Piao W, Vogel SN, Medvedev AE. The Asp299Gly polymorphism alters TLR4 signaling by interfering with recruitment of MyD88 and TRIF. *J Immunol* (2012) 188(9):4506–15. doi: 10.4049/jimmunol.1200202
- Long H, O'Connor BP, Zemans RL, Zhou X, Yang IV, Schwartz DA. The Toll-like receptor 4 polymorphism Asp299Gly but not Thr399Ile influences TLR4 signaling and function. *PLoS One* (2014) 9(4):e93550. doi: 10.1371/journal.pone.0093550
- Wolf J, Weinberger B, Arnold CR, Maier AB, Westendorp RG, Grubeck-Loebenstein B. The effect of chronological age on the inflammatory response of human fibroblasts. *Exp Gerontol* (2012) 47:749–53. doi: 10.1016/j.exger.2012.07.001
- Wurfel MM, Park WY, Radella F, Ruzinski J, Sandstrom A, Strout J, et al. Identification of High and Low Responders to Lipopolysaccharide in Normal Subjects: An Unbiased Approach to Identify Modulators of Innate Immunity. *J Immunol* (2005) 175:2570–8. doi: 10.4049/jimmunol.175.4.2570

39. Kandasamy S, Kerr DE. Genomic analysis of between-cow variation in dermal fibroblast response to lipopolysaccharide. *J Dairy Sci* (2012) 95(7):3852–64. doi: 10.3168/jds.2011-5251
40. Altman JB, Taft J, Wedeking T, Grubera CN, Holtmannspötter M, Pielher J, et al. Type I IFN is siloed in endosomes. *Proc Natl Acad Sci U S A* (2020) 117(30):17510–2. doi: 10.1073/pnas.1921324117
41. Zhang SY, Jouanguy E, Zhang Q, Abel L, Puel A, Casanova JL. Human inborn errors of immunity to infection affecting cells other than leukocytes: from the immune system to the whole organism. *Curr Opin Immunol* (2019) 59:88–100. doi: 10.1016/j.coi.2019.03.008
42. West NR. Coordination of Immune-Stroma Crosstalk by IL-6 Family Cytokines. *Front Immunol* (2019) 10:1093. doi: 10.3389/fimmu.2019.01093

Conflict of Interest: The authors declare that the research was conducted in the absence of any commercial or financial relationships that could be construed as a potential conflict of interest.

Copyright © 2021 Chansard, Dubrulle, Poujol de Molliens, Falanga, Stephen, Hasan, van Zandbergen, Aulner, Shorte, David-Watine and the Milieu Intérieur Consortium. This is an open-access article distributed under the terms of the Creative Commons Attribution License (CC BY). The use, distribution or reproduction in other forums is permitted, provided the original author(s) and the copyright owner(s) are credited and that the original publication in this journal is cited, in accordance with accepted academic practice. No use, distribution or reproduction is permitted which does not comply with these terms.